Carbohydrate Polymers 118 (2015) 1–8

Contents lists available at ScienceDirect

Carbohydrate Polymers

journal homepage: www.elsevier.com/locate/carbpol

A comparative study on properties of micro and nanopapers produced from cellulose and cellulose nanofibres

A. Mtibe[a,b,*], Linda Z. Linganiso[a,*], Aji P. Mathew[c], K. Oksman[c], Maya J. John[a,b], Rajesh D. Anandjiwala[a,b]

[a] CSIR Materials Science and Manufacturing, Polymers and Composites Competence Area, Nonwovens and Composites Research Group, PO Box 1124, 4 Gomery Avenue, Summerstrand, Port Elizabeth 6000, South Africa
[b] Department of Textile Science, Faculty of Science, Nelson Mandela Metropolitan University, PO Box 1600, Port Elizabeth 6000, South Africa
[c] Division of Manufacturing and Design of Wood and Bionanocomposites, Luleå University of Technology, SE-97187 Luleå, Sweden

ARTICLE INFO

Article history:
Received 16 August 2014
Received in revised form
30 September 2014
Accepted 3 October 2014
Available online 17 October 2014

Keywords:
Maize stalk residues
Cellulose nanocrystals
Cellulose nanofibres
Cellulose nanopapers
Micropapers

Chemical compounds studied in this article:
Sodium hydroxide (PubChem CID: 14798)
Sodium hydroxide (PubChem CID: 14797)
Sodium chlorite (PubChem CID: 23668197)
Sulphuric acid (PubChem CID: 1118)

ABSTRACT

Cellulose nanocrystals (CNCs) and cellulose nanofibres (CNFs) were successfully extracted from cellulose obtained from maize stalk residues. A variety of techniques, such as Fourier transform infrared (FTIR) spectroscopy, scanning electron microscopy (SEM), X-ray diffraction (XRD) and thermogravimetric analysis (TGA) were used for characterization and the experimental results showed that lignin and hemicellulose were removed to a greater extent by following the chemical methods. Atomic force microscopy (AFM) results confirmed that the diameters of CNCs and CNFs were ranging from 3 to 7 nm and 4 to 10 nm, respectively, with their lengths in micro scale. CNCs suspension showed a flow of birefringence, however, the same was not observed in the case of suspension containing CNFs. XRD analysis confirmed that CNCs had high crystallinity index in comparison to cellulose and CNFs. Nanopapers were prepared from CNCs and CNFs by solvent evaporation method. Micropapers were also prepared from cellulose pulp by the same technique. Nanopapers made from CNFs showed less transparency as compared to nanopapers produced from CNCs whereas high transparency as compared to micropaper. Nanopapers produced from CNFs provided superior mechanical properties as compared to both micropaper and nanopapers produced from CNCs. Also, nanopapers produced from CNFs were thermally more stable as compared to nanopapers produced from CNCs but thermally less stable as compared to micropapers.

1. Introduction

The depletion of petroleum based resources and attendant environmental problems such as global warming, have shown a great interest in developing environmentally sustainable materials (Miao et al., 2014). Biobased materials could be used as suitable replacement to petroleum based materials to overcome environmental problems. These materials offer advantages, such as renewability, biodegradability and environmental friendliness. They are composed of cellulose, lignin, hemicelluloses and the extractives (Neto, Silvério, Oliveira, & Pasquini, 2013).

Cellulose is the most abundant natural homopolymer and renewable resource on earth. It is made up of bundles of fibrils called microfibrils. However, individual fibril consists of crystalline region and amorphous domains. CNCs are the rod shaped crystalline part remained after the removal of the amorphous domains (Rosa et al., 2010; Rosli, Ahmad, & Abdullah, 2013).

There are several methods available for extracting CNCs, which include enzyme or microbial hydrolysis (Satyamurthy & Vigneshwaran, 2013) and acid hydrolysis (Neto et al., 2013). However, sulphuric acid hydrolysis is one of the preferred methods for the extraction of CNCs from natural biobased materials due to the formation of sulphate charges on the surface of the material which helps in stabilizing the suspension (Fahma, Iwamoto, Hori, Iwata, & Takemura, 2011). On the other hand, CNFs are extracted by means of mechanical treatment such as high shear homogenization (Zhao et al., 2013), mechanical grinding (Yousefi et al., 2013), a combination of mechanical actions and enzyme hydrolysis (Qing et al., 2013), and a combination of mechanical actions and chemical method (Qing et al., 2013).

* Corresponding authors at: Nonwovens and Composites Research Group, CSIR Materials Science and Manufacturing, Polymers and Composites Competence Area, PO Box 1124, 4 Gomery Avenue, Summerstrand, Port Elizabeth 6000, South Africa. Tel.: +27 415083251; fax: +27 415083277.
E-mail addresses: mtibe.asanda@gmail.com (A. Mtibe), LLinganiso@csir.co.za (L.Z. Linganiso).

http://dx.doi.org/10.1016/j.carbpol.2014.10.007
0144-8617/

The diameters of these CNCs and CNFs are in the nano scale (<100 nm) range with the lengths in micron size (Rosa et al., 2010; Satyamurthy & Vigneshwaran, 2013; Fahma et al., 2011; Zhao et al., 2013). Because of the improved properties of CNCs and CNFs, such as high aspect ratio, high surface area per unit volume, high strength and stiffness as compared to those of fibres, they are reported to provide improved properties of the composites when used as reinforcing elements (Chen, Liu, Chang, Cao, & Anderson, 2009).

Cellulose nanomaterials are usually extracted from natural fibres, such as flax (Cao, Dong, & Li, 2007), agave (Rosli et al., 2013), kenaf (Kargarzadeh et al., 2012) and sisal fibres (Siqueira, Tapin-Lingua, Bras, Perez, & Dufresne, 2010), etc. Very few studies have reported the extraction of cellulose nanomaterials from maize stalk residues. Maize is abundantly produced in South Africa and is planted all over the country annually in rainy seasons. Approximately 8 million tons of maize is produced yearly in South Africa in approximately 3.1 million hectares (ha) of land (Du Plessiss, 2003). In developing countries like South Africa and other African countries maize serves as a staple food in the majority of population. The agricultural sector produces maize for the purpose of economic growth and after harvesting, maize stalk residues remain in the field, because they do not have any direct use and therefore are underutilized (Du Plessiss, 2003). Maize stalk residues are used in low-value products, such as animal feed or disposed-off by incineration or dumped in waste sites due to the lack of space and little knowledge about possible value addition on such agricultural wastes (Brent, Rohwer, Friedrich, & Von Blottnitz, 2002). In this study, CNFs and CNCs are extracted from maize stalk residues by supermass colloider and acid hydrolysis, respectively.

CNFs are usually utilized to prepare nanopapers or they are used for the development of composite materials in most cases (Sehaqui, Liu, Zhou, & Berglund, 2010). The process of preparing nanopapers is analogous to the traditional papermaking process; the only difference is that nanopapers are made up of high aspect ratio nanomaterials in comparison to conventional paper (Sehaqui et al., 2010; Henriksson, Berglund, Isaksson, Lindström, & Nishino, 2008). The common processes of preparing nanopapers are: solvent evaporation method (Wu et al., 2013; Fukuzumi, Saito, & Isogai, 2013) and filtration accompanied with hot pressing method (Missoum, Martoïa, Belgacem, & Bras, 2013; Wang, Li, & Zhang, 2013). CNFs in wet state are in gel-like form and the fibres are normally in an entangled state. During water evaporation process the individual fibres attract each other by means of capillary action and create hydrogen bonding amongst them. Nanopapers have been reported to exhibit high strength and stiffness, excellent optical transparency, and low thermal expansion (Sehaqui et al., 2010).

Various studies have shown that nanopapers prepared from CNFs (from various sources) using mechanical grinding technique have high tensile strength and high tensile modulus (Yousefi et al., 2013; Qing et al., 2013; Wang et al., 2013). Qing et al. (2013) reported that the tensile strength and tensile modulus of nanopapers prepared from bleached eucalyptus Kraft pulp was about 123 MPa and 7 GPa, respectively. The findings obtained by Yousefi et al. (2013) showed that nanopapers prepared from bacterial cellulose and canola straw had tensile strength and tensile modulus of 185 and 114 MPa and 17.3 and 13.6 GPa, respectively. Also, Wang et al. (2013) prepared nanopapers from waste corrugated paper pulp by oven drying and hot pressing method. They found that the tensile strength and tensile modulus of nanopapers prepared by oven drying and hot pressing nanopapers were about 140 and 152 MPa and 6.5 and 9.26 GPa.

The main objective of this study was to extract cellulose from maize stalk residues and to characterize it by FTIR, ESEM, TGA and XRD techniques. Another objective of this study was to produce high quality CNFs and CNCs from cellulose obtained maize stalk residues using supermass colloider and acid hydrolysis. The morphological features of the CNFs and CNCs will be determined by AFM. Also, their dispersion in suspensions will be determined by light polarized microscopy. The obtained CNFs and CNCs were used to develop nanopapers and their mechanical, thermal properties and optical transparency were investigated. Micropaper was prepared from extracted cellulose pulp and used as a control for comparison.

2. Materials and methods

2.1. Materials

The post harvested maize stalks residues were supplied by a farm in Cofimvaba in Eastern Cape, South Africa. They were grounded into a coarse powder by Hamermeul. Sodium hydroxide (NaOH) pellets, potassium hydroxide (KOH) and sulphuric acid (H_2SO_4) of 99.9%, 85% and 98% purity, respectively, were obtained from Minema Chemicals, South Africa. Sodium chlorite ($NaClO_2$) of 80% purity was purchased from Sigma Aldrich, South Africa.

2.2. Experimental methods

2.2.1. Extraction of cellulose

The post-harvested maize stalks were grounded into a coarse powder by Hamermeul. The maize stalk powder was then weighed and dried in an oven at 50 °C overnight and treated with 1.5% NaOH, 1.5% $NaClO_2$, and 1.5% KOH, respectively, for 1 h. Each treatment was repeated four times with repeated washes using deionized water to remove excess chemicals and to achieve a neutral pH. The schematic diagram of the extraction of cellulose from maize stalk residues and extraction of cellulose nanocrystals and nanofibres is shown in Fig. 1.

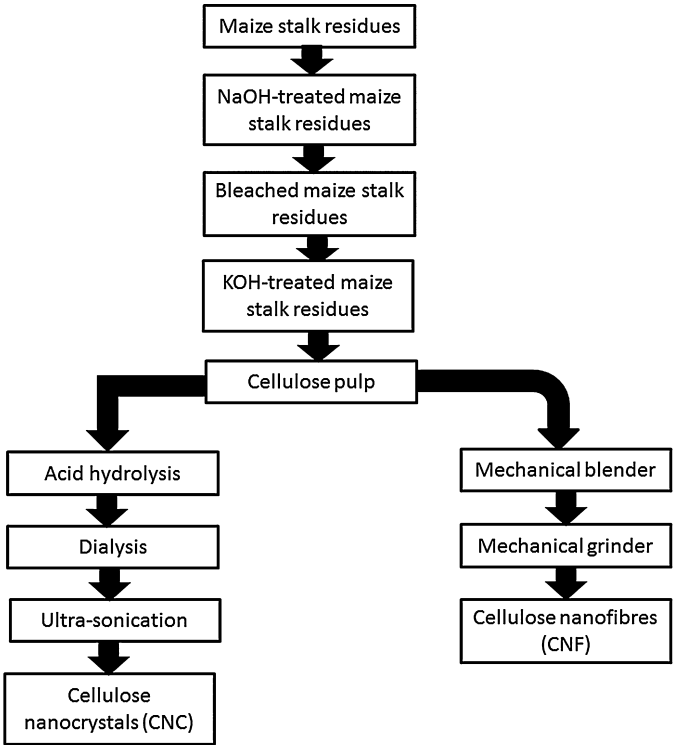

Fig. 1. Extraction of cellulose nanocrystals and nanofibres from cellulose obtained from maize stalk residues.

2.2.2. Extraction of CNFs

Cellulose pulp (2%) was agitated in a mechanical blender [Silverson L4RT (England)] at 35000 rpm for 15 min. Then, the dispersed suspension was ground using a supermass colloider [MKCA6-3 (Masuko Sangyo Co, Ltd., Japan)] at a speed of 1500 rpm for 20 min until a gel-like substance was achieved.

2.2.3. Extraction of CNCs

Cellulose obtained from maize stalk residues after KOH treatment was hydrolyzed using 50% acid concentration under a strong agitation of 1000 rpm, at 40 °C for 30 min, keeping acid/pulp ratio at 20:1 (ml/g). The hydrolysis process was terminated by adding 10-folds (1000 ml) of deionized (DI) water. The suspensions were then centrifuged at 8000 rpm for 10 min and dialyzed with deionized water for 3 days until the pH was neutral. Subsequently, the suspension was dispersed by ultrasonication for 1 min. Finally, the suspensions were stored in a refrigerator at 4 °C with the addition of few drops of chloroform to avoid fungal growth.

2.2.4. Preparation of nanopapers and micropapers

Cellulose nanopapers and micropapers were prepared by solvent evaporation of 0.5% by weight of CNCs/CNFs/cellulose pulp. The well-dispersed suspensions were poured in petri dishes with a diameter of 195 mm and the water was allowed to evaporate at room temperature for 48 h. Afterwards, the nanopapers and micropapers were ready to be transferred to a standard climate (20 °C and 50% relative humidity) for final conditioning before further characterization.

2.3. Characterization methods

2.3.1. Morphology studies

FEI Quanta 200 (FEI Co., Eindhoven, the Netherlands) environmental scanning electron microscope (ESEM) operated at an accelerating voltage of 20 kV was utilized to capture images. The samples of the untreated and chemical treated (NaOH, $NaClO_2$ and KOH) maize stalks were coated by gold prior to ESEM analysis. Cross section of maize stalk was measured using an Olympus CX31 light microscopy equipped with CC-12 soft imaging system, Olympus U-SPT and U-PMTVC 3102205, Japan. Furthermore, atomic force microscope (AFM), [Veeco Multi Mode instrument equipped with nanoscope V controller] was utilized to measure the dimensions of CNCs and CNFs. For the analysis of CNCs and CNFs, a droplet of the aqueous suspension containing CNCs and CNFs was dried on a mica surface prior to capturing images on AFM.

2.3.2. Birefringence studies

The aliquots of CNCs and CNFs were placed in sample vials. The vials were placed in front of a source of polarized light and photographed using a DX Nikon camera.

2.3.3. Thermal stabilities

Thermogravimetric analysis was carried out on a thermogravimetric analyser (Perkin Elmer, Buckinghamshire, UK) at a heating rate of 10 °C/min using nitrogen as purge gas. The TGA programme was conditioned to increase the temperature linearly from room temperature to 700 °C under nitrogen flow. The temperature of the sample was monitored and the loss in weight of the sample was expressed in terms of percentage weight loss.

2.3.4. Crystallinity

The X-ray diffraction (XRD) profiles of the untreated and chemical treated (NaOH, $NaClO_2$, and KOH) maize stalk residues, CNCs and CNFs were measured using BRUKER AXS (Germany) X-ray Diffractometer D8 Advance equipped with PSD (Position sensitive detector) Vantec-1 detector and Cu-$K\alpha$ radiation ($\lambda K\alpha_1 = 1.5406$ Å). Scattering radiation was detected in a $2\theta = 5$–90° at a rate of 1 s per step. The amorphous peak and crystallinity peak are usually observed in XRD pattern. To quantify XRD results, crystallinity index (CI) was determined from following two methods:

(1) The XRD peak height method: In this method CI is calculated from the height of the 0 0 2 peak (I_{002}) and the height of the minimum (I_{AM}) between the 0 0 2 peak and the 0 0 1 peak.
(2) The deconvolution method: In this method the sample crystallinity was determined by taking into account the amorphous and crystalline contributions to the diffraction intensity (Segal, Greely, Martin, & Conrad, 1959).

Where $I_{(002)}$ is the counter reading at peak intensity, 2θ angle close to 22°, representing crystalline material and $I_{(AM)}$ is the counter reading at peak intensity, 2θ angle close to 18°, representing amorphous material in cellulose fibres.

2.3.5. Chemical analysis

The spectra of the untreated and chemical treated maize stalks were obtained using FTIR-ATR Perkin-Elmer 4000. All samples were scanned over a range of 4000–600 cm^{-1} with an average of 4 scans with a resolution of 4 cm^{-1}.

2.3.6. Optical properties

The optical transmittances of nanopapers made from CNCs and CNFs and micropapers were measured at a wavelength range from 300 to 900 nm using Perkin Elmer Lambda 35 UV/vis Spectrometer. Rectangular specimens of dimensions 40 mm × 10 mm (length × thickness) were measured with a scan speed of 240 nm/min and three replicates of each sample were used.

2.3.7. Tensile properties

The tensile tests of micropapers and nanopapers made from cellulose pulp, CNCs and CNFs were performed on a universal testing machine, Shimadzu Autograph AG-X (Japan); with a load cell of 1 kN and the gauge length of 20 mm. A frame was used to support the specimens in order to prevent them from being damaged by the grips. The elastic modulus was calculated from the initial part of the gradient from stress-strain curves. For each type of sample, at least seven test specimens were tested and the average values were presented.

3. Results and discussions

3.1. Purification of maize stalk residues

The weight of cellulose obtained after chemical treatment was measured and the results confirmed that only 36% yield was achieved. Alkali and bleaching treatments are used to remove the amorphous lignin and hemicelluloses which are cementing the cellulose (Henrique, Silvério, Neto, & Pasquini, 2013). Dilute alkali treatment solubilize lignin and hemicellulose, while bleaching treatment removes lignin (Dufresne, 2012).

3.1.1. FTIR analysis

The FTIR spectra of the untreated and chemical treated (NaOH, $NaClO_2$ and KOH) maize stalks are displayed in Fig. 2. A broad peak at 3314 cm^{-1} corresponds to the hydroxyl group (OH) of the cellulose fibre and a strong peak at 2885 cm^{-1} is assigned for C—H stretching vibrations in hemicellulose and cellulose. The peak at 1725 cm^{-1} is observed only in the spectrum of the untreated maize stalks, this peak represents C=O stretching vibrations of the acetyl and uronic ester groups of the hemicellulose or ester linkage of carboxylic group of ferulic and *p*-coumaric acids of hemicellulose or lignin (Neto et al., 2013; Li et al., 2009). This peak disappeared

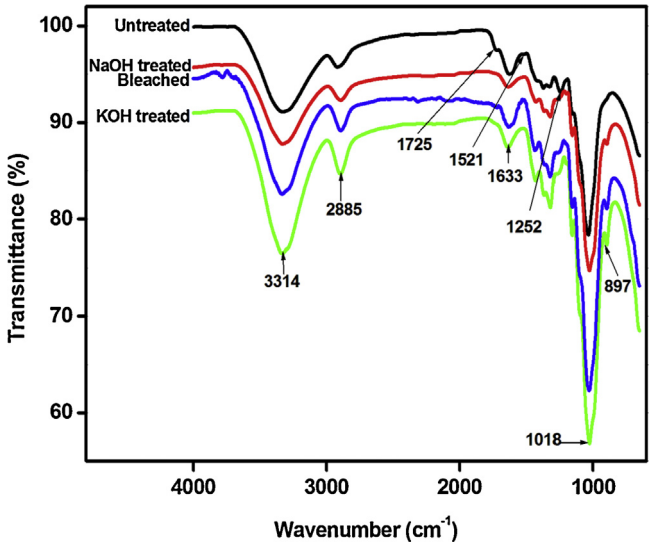

Fig. 2. FTIR spectra of the untreated and chemical treated (NaOH, $NaClO_2$ and KOH) maize stalk residues.

after chemical treatment; which is an indication of the removal of hemicellulose and lignin from the untreated maize stalks after chemical treatment. The absorption band at 1633 cm^{-1}, in all spectra, corresponds to water absorption which is attributed to the bending modes of water molecules present in the cellulose material (Li et al., 2009; Haafiz, Eichhorn, Hassan, & Jawaid, 2013). The small peak at 1521 cm^{-1} is assigned to aromatic C=C stretching vibrations in lignin while the band at 1252 cm^{-1} corresponds to =C—O—C, which is commonly seen when =C—O— in ether, ester and phenol groups are present (Silvério, Neto, Dantas, & Pasquini, 2013). The disappearance of these peaks after chemical treatment indicates the complete removal of lignin. The absorption band at 1018 cm^{-1} corresponds to C—O—C stretching vibrations and a peak at 897 cm^{-1} corresponds to C—H rock vibrations of cellulose material; these peaks were observed in all spectra (Li et al., 2009) (Fig. 2).

3.1.2. Morphological studies

The cross sectional area of maize stalk is shown in Fig. 3. Maize stalks contain pith, tracheid xylem, phloem and sclerenchyma. The pith is made up of parenchyma or chlorenchyma tissue and the role of pith is for food storage and it is vanished when the maize plant grows old (http://users.rcn.com/jkimball.ma.ultranet/BiologyPages/S/Stems.html (30-07-2014)). Tracheid xylem lifts water, dissolves mineral salts and cools the leaves of maize

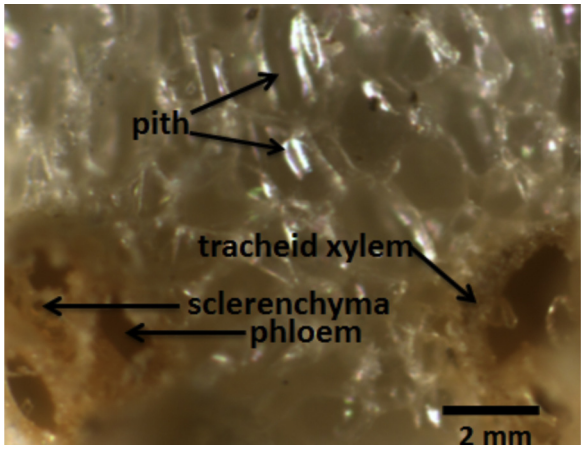

Fig. 3. Cross-sectional area of the untreated maize stalk residue.

(http://users.rcn.com/jkimball.ma.ultranet/BiologyPages/S/Stems.html (30-07-2014)). The role of phloem to the plant is to transport nutrients produced during photosynthesis (Sheltami, Abdullah, Ahmad, Dufresne, & Kargarzadeh, 2012). Sclerenchyma is utilized to make seeds hard, store starch granules and assist in water transportation to the entire plant (http://www.botany.uwc.ac.za/sci_ed/grade10/plant_tissues/sclerenchyma.htm (30-07-2014)).

The surface morphologies of the untreated and chemical treated (NaOH, $NaClO_2$ and KOH) maize stalks were investigated by ESEM (Fig. 4A–D). The chemical treatment of the maize stalks was anticipated to enhance the morphological changes in the material. The untreated maize stalks displayed a bundle of fibres which were bonded together by non-cellulosic components (lignin, hemicellulose and extractives) (Fig. 4A). During alkali treatment, some of the non-cellulosic components were removed. Alkali treatment dissolves hemicellulose and induces defibrillation of fibre bundles (Rosli et al., 2013; Kargarzadeh et al., 2012). The surface of maize stalks after alkali treatment became rougher (Fig. 4B) as compared to the untreated maize stalks. Bleaching treatment in Fig. 4C delignifies fibres and enhances further defibrillation of fibre bundles into individual fibres. It is worth noting that the diameters of the individual fibres were reduced after bleaching as compared to the untreated and NaOH treated maize stalks. KOH treatment further removes hemicellulose resulting in further defibrillation and size reduction (Fig. 4D). These results are in agreement with the FTIR results (Fig. 2).

3.1.3. XRD analysis

The XRD profiles of the untreated and chemical treated (NaOH, $NaClO_2$ and KOH) maize stalks are shown in Fig. 5. All samples displayed four reflection peaks of cellulose I at $2\theta = 15.7$, 22.6, 34.9, and 46.4°, respectively. The reflection peak at $2\theta = 22.56°$ becomes more intense upon chemical treatment; this indicates the increase in crystallinity of the material. The untreated maize stalks as anticipated displayed a low crystallinity index (Table 1) as compared to chemically treated (NaOH, $NaClO_2$ and KOH) samples. This could be due to the fact that the untreated maize stalks contain non-cellulosic amorphous materials (lignin, hemicellulose, pectin and waxes) (Silvério et al., 2013). In general, crystallinity index increases upon chemical treatment (Silvério et al., 2013; Neto et al., 2013) presumably due to the removal of non-cellulosic amorphous material induced by chemical treatments. Crystallinity index increases from the untreated maize stalks to cellulose material obtained after chemical treatment. Crystallinity index after NaOH treatment increased by 10.2%, after bleaching it increased by 12.3% and after KOH treatment, it increased by 16.7%, respectively. These findings correlate with the results obtained from FTIR and SEM analysis.

The extraction methods used to extract CNCs (acid hydrolysis) and CNFs (mechanical grinding) did not change the crystal structure of the original cellulose material. CNCs displayed the highest crystallinity index relative to CNFs. This confirms the hypothesis that the preparation of CNCs by acid hydrolysis dissolves amorphous domains of the cellulose fibre and thereby releases rod shaped single crystallites which increase the crystallinity of cellulose (Silvério et al., 2013; Neto et al., 2013). CNFs had low crystalline index relative to CNCs and cellulose pulp. This is probably due to the fact that the mechanical grinding grinds fibres randomly with high forces created between the silicone grinding stones and thereby destroying the crystalline domains. This could lead to the decrease in crystallinity index (Yousefi et al., 2013). Similar observations were reported in other studies (Yousefi et al., 2013; Qing et al., 2013).

3.1.4. Thermal stability analysis

Thermogravimetric analysis (TGA) and differential thermograms (DTG) of the untreated and chemical treated (NaOH, $NaClO_2$

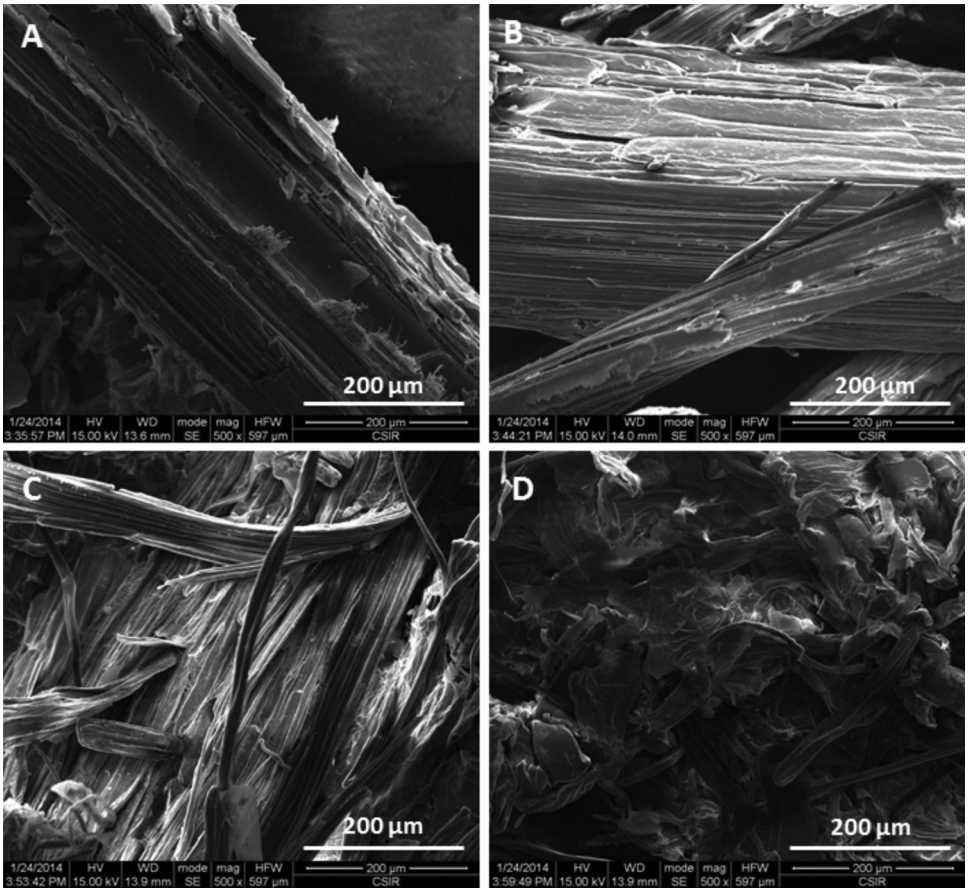

Fig. 4. ESEM images of (A) untreated, (B) NaOH treated, (C) $NaClO_2$ and (D) KOH treated maize stalk residues.

and KOH) maize stalks are shown in Fig. 6A and B. The TG and DTG analyses revealed a shift in decomposition peaks between the untreated and chemical treated maize stalks. The DTG curve of the untreated maize stalks displayed a small hump at 191 °C next to a main degradation peak. This could be due to the presence of non-cellulosic components i.e. hemicellulose (Li et al., 2009).

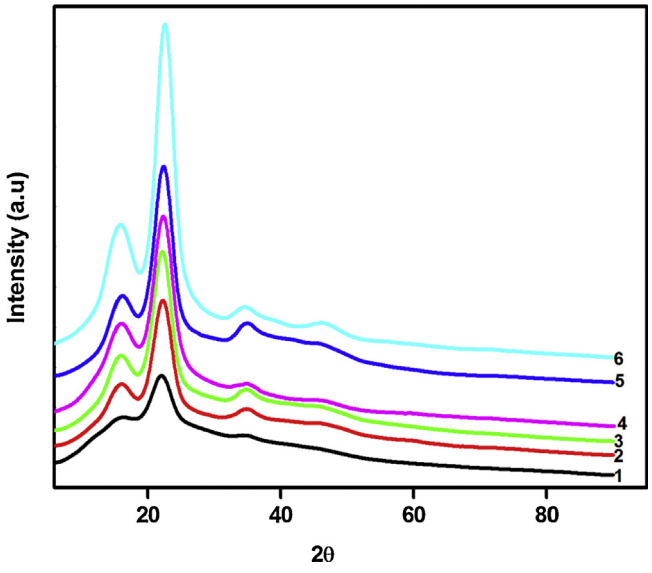

Fig. 5. X-ray diffraction patterns of (1) untreated maize stalk, (2) NaOH treated maize stalks, (3) bleached maize stalks, (4) CNFs, (5) KOH treated maize stalks and (6) CNCs.

After chemical treatment, the small hump disappeared (Fig. 6B), which indicate the removal of non-cellulosic components. Also, the untreated maize stalks displays an early decomposition, starting at 222 °C to 365 °C but the main decomposition peak was found to be at 310 °C which corresponds to the degradation of cellulose (Li et al., 2009). From the DTG curve (Fig. 6B) it was noticed that after chemical treatment the prominent peak shifted to higher temperatures with the increasing intensity of the peaks. The main decomposition peak for NaOH, $NaClO_2$ and KOH treated maize stalks was 336 °C, 348 °C and 352 °C, respectively. These peaks correspond to the degradation of cellulose (Li et al., 2009). Silvério et al. (2013) investigated thermal analysis of corncob and corncob treated with NaOH and $NaClO_2$. They found that the untreated corncob displayed a maximum degradation temperature of 290 °C, whereas the same for treated corncob was found to be 345 °C. It was also noticed that the untreated maize stalks showed higher char residue as compared to the chemical treated maize stalks. This could be due to the presence of lignin or cellulose–lignin complex. Lignin starts decomposition at 160 °C and it extends up to 600 °C.

Table 1
Crystallinity indices of the untreated and chemical treated (NaOH, $NaClO_2$, and KOH) maize stalks, CNFs and CNCs.

Sample	Crystallinity (%)
Untreated maize stalks	53.8
NaOH treated maize stalks	64.0
Bleached maize stalks	66.1
KOH treated maize stalks	70.5
CNFs	66.4
CNCs	72.6

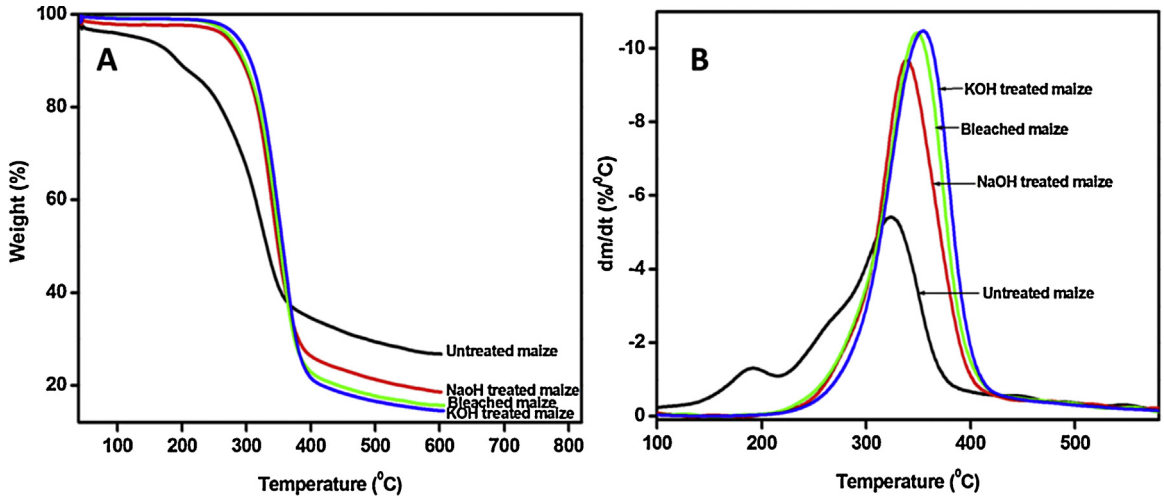

Fig. 6. (A) and (B) are TGA and DTG profiles of the untreated and chemical treated maize stalks.

3.2. Extraction of cellulose nanocrystals and nanofibres

3.2.1. AFM and birefringence studies

Fig. 7A and C display AFM images of CNCs and CNFs. The diameters of both CNCs and CNFs were in nano scale and their lengths in micron scale. CNFs displayed a web structure with diameters ranging from 4 to 10 nm while CNCs exhibit a rod like shape with diameters ranging from 3 to 7 nm and the lengths were in microns ranging from 150 to 450 nm. The aspect ratios of CNCs were estimated to be ranging between 50 and 64. It is worth to note that these findings are in agreement with the results reported by Silvério et al. (2013). They obtained CNCs with an average diameter of 4.15 ± 10.8 nm, average length of 210.8 ± 44.2 nm and average aspect ratio of 53.4 ± 15.8, respectively.

Fig. 7B and D illustrate the flow birefringence of suspensions containing CNCs and CNFs in water. The presence of birefringence is the evident of the good dispersion of materials in water (Silvério et al., 2013). It has been reported that birefringence result from a structural anisotropy form of cellulose and flow anisotropy resulting from the alignment of the nanocrystals under flow (Silvério et al., 2013; Neto et al., 2013). No birefringence (static or flow) was observed for CNFs suspension (Fig. 7D). This could be due to the structure of CNFs (Fig. 7C) which tends to agglomerate due to the lack of negative charges on the surface of CNFs fibrils (Qing et al., 2013). Suspension containing CNCs (Fig. 7B) shows a flow of birefringence which is an indication of isolated nanocrystals and good dispersion (Silvério et al., 2013; Neto et al., 2013). This could be attributed to the presence of negative sulphate charges on the surface of CNCs which stabilize the suspension containing CNCs. The birefringence in suspension containing CNCs (Fig. 7B) was not strong enough; this could be due to the presence of larger particles in the suspension which were not hydrolyzed therefore resulting in weak birefringence (Oksman, Etang, Mathew, & Jonoobi 2011).

3.3. Characterization of nanopapers (made from CNCs and CNFs) and micropapers

3.3.1. Thermal stability analysis

Fig. 8 A and B display TG and DTG profiles of micropapers and nanopapers made from CNCs and CNFs. Initially, a slight weight loss was observed at low temperatures from 50 to 100 °C. This weight loss could be attributed to the evaporation of moisture (Yousefi et al., 2013; Kargarzadeh et al., 2012). Cellulose micropapers and nanopapers made from CNFs displayed two steps degradation. The first rapid step was due to the degradation of cellulose, either by depolymerization, dehydration, and decomposition of glycosidic bonds (Yousefi et al., 2013) at temperatures 320 °C and 330 °C, respectively. The second degradation step was due to the oxidation and breakdown of charred residues at 430 °C and 450 °C (Yousefi et al., 2013). But, nanopapers prepared by CNCs displayed three

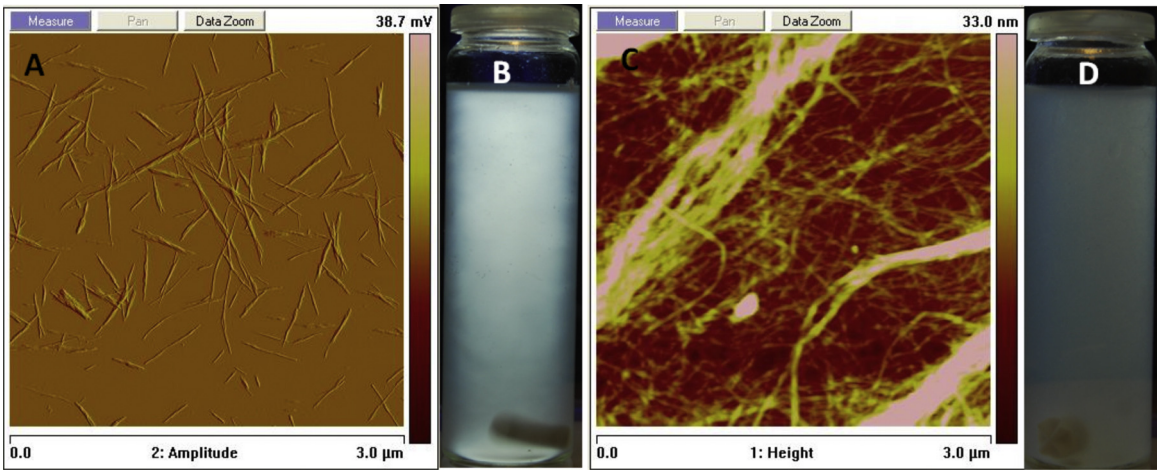

Fig. 7. (A) and (C) shows AFM images of CNCs and CNFs and (B) and (D) are birefringence of suspensions containing CNCs and CNFs.

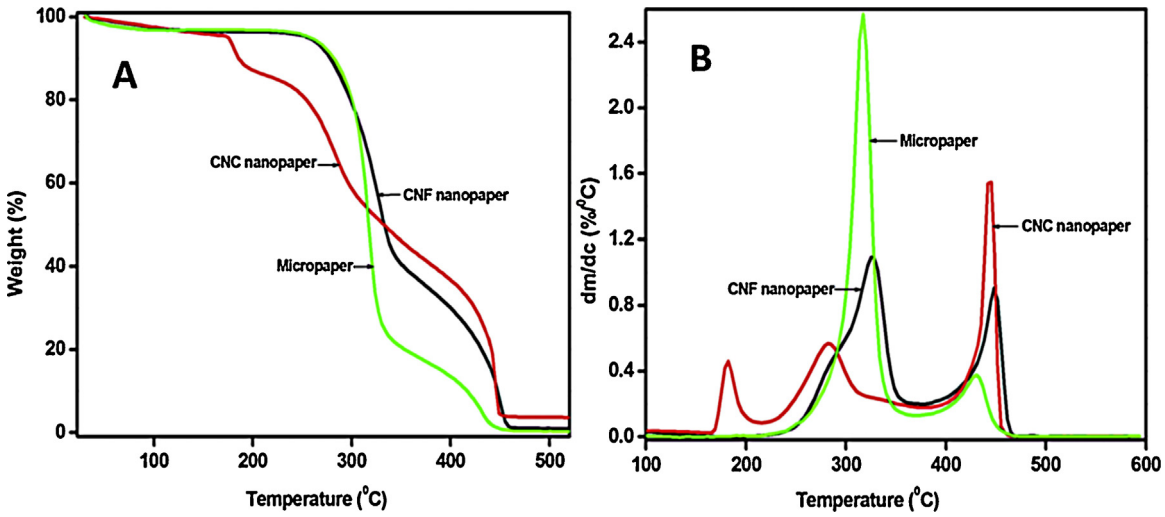

Fig. 8. (A) TGA and (B) DTG curves of micropapers and nanopapers prepared by CNCs and CNFs.

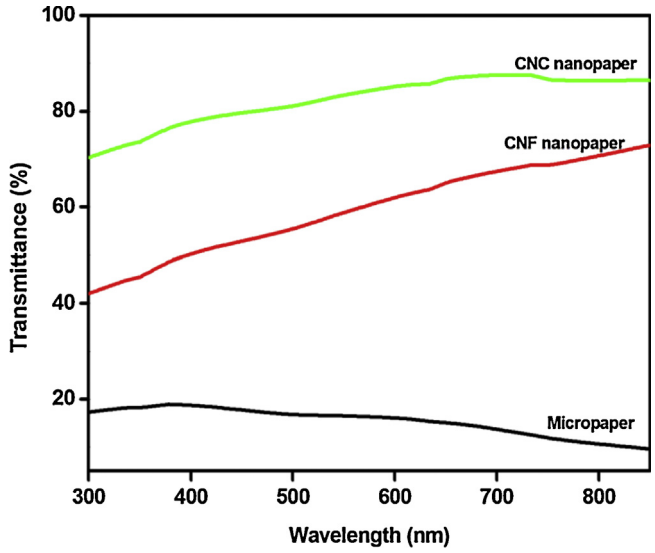

Fig. 9. UV–vis transmittance spectra of micropapers and nanopapers prepared by CNCs and CNFs.

steps degradation (Fig. 8B). The first degradation process occurred at 190 °C corresponding to the degradation of highly accessible sulphated regions (Silvério et al., 2013). The second degradation peak at 290 °C corresponds to the degradation of crystalline regions which were not attacked by sulfuric acid (Silvério et al., 2013). The third degradation step at 450 °C corresponds to the oxidation and breakdown of charred residues to lower molecular weight gaseous materials (Yousefi et al., 2013; Kargarzadeh et al., 2012).

3.3.2. Transparency studies

The UV–vis transmittance spectra of the nanopapers prepared from CNCs, nanopapers prepared from CNFs and micropapers in a visible wavelength range of 300–900 nm are shown in Fig. 9. Nanopapers prepared from CNCs were the most transparent, followed by nanopapers prepared by CNFs and then micropapers. The transparency results of UV–vis transmittance are in agreement with optical transparency photographs of nanopapers and micropaper (Figure not shown). However, the difference in optical transparency can be related to the structures and dimensions of materials used to prepare micropaper and nanopapers. For example, CNFs have a web structure which increases light scattering, so hinders transparency of the nanopapers prepared by CNFs (Qing et al., 2013). The high transparency of the nanopapers prepared from CNCs might also depend on the uniform nano-sized material of CNCs.

3.3.3. Mechanical properties

Table 2 displays tensile strength, tensile modulus, and strain at break of the micropapers and nanopapers prepared from CNFs and CNCs. The mechanical properties of the nanopapers were compared to micropapers. The results obtained in this study revealed that the nanopapers prepared from CNFs provided high tensile properties in comparison to micropapers and nanopapers prepared from CNCs. This could be due to the fact that CNFs have high aspect ratio which enhances tensile properties (Iwatake, Nogi, & Yano, 2008). In addition, the interconnected network of fibrils in CNFs helps the stress transfer from fibril-to-fibril (Huang & Netravali, 2009). Nanopapers prepared from CNFs exhibits high tensile strength of 95.56 MPa in comparison to that of 32.77 MPa for nanopapers prepared CNCs. CNCs (Fig. 7A) does not have interconnected fibrilliar network which is reported to improve tensile properties (Iwatake et al., 2008). The tensile modulus of nanopapers prepared by CNFs was also high in comparison to nanopapers prepared from CNCs. The tensile modulus of nanopapers prepared from CNFs and nanopapers prepared from CNCs were 8.759 and 4.325 GPa, respectively. The strain at break also followed the same trend as tensile strength and tensile modulus of nanopapers and micropapers. The tensile properties of the micropapers were low as compared to nanopapers. Similar observations were reported by Yousefi et al. (2013). The lower mechanical properties of nanopapers prepared from CNCs is unexpected and is difficult to explain.

Table 2
Shows tensile strength, tensile modulus, and strain at break of the micropapers and nanopapers prepared from CNFs and CNCs.

Sample	Tensile strength (MPa)	Tensile modulus (GPa)	Strain at break (%)
Micropaper	3.28 ± 0.27	0.2295 ± 0.057	1.57 ± 0.058
Nanopapers prepared from CNCs	32.77 ± 1.7	4.325 ± 1.4	1.6 ± 0.46
Nanopapers prepared from CNFs	95.56 ± 2.7	8.759 ± 0.79	2.325 ± 0.25

4. Conclusions

Cellulose fibres were successfully extracted from maize stalk residues. The removal of cementing materials such as lignin, hemicellulose, and extractives were confirmed by FTIR, ESEM, XRD and TGA techniques. The web structure of CNFs with diameters ranging from 4 to 10 nm and length in microns were successfully extracted from cellulose obtained from maize stalk. The rod shaped CNCs with diameters ranging from 3 to 7 nm, lengths ranging from 150 to 450 nm and aspect ratios ranging from 50 to 64 were also successfully extracted from cellulose obtained from maize stalk as indicated by AFM results. XRD analysis showed that CNCs and CNFs had a crystallinity index of 72.6% and 66.4%, respectively. As a result of mechanical grinding, CNFs showed lower crystallinity index of 66.4% as compared to both CNC (72.6%) and extracted cellulose pulp (70.5%), due to the fact that the grinding process destroys the crystalline domain of cellulose fibres. Also, suspensions containing CNCs showed a flow of birefringence and the same was not observed for suspensions containing CNFs. Nanopapers prepared from CNFs was more transparent in comparison to micropapers whereas it was less transparent in comparison to nanopapers prepared from CNCs. This was undoubtedly due to the network structure of CNFs which increases the light scattering and hinders transparency of the material. Furthermore, the web shape CNFs facilitates the stress transfer from fibril-to-fibril, and therefore increases the mechanical properties of the material. It was observed that nanopapers prepared from CNFs had high thermal stability in comparison to nanopapers prepared by CNCs and lower thermal stability as compared to micropapers.

Acknowledgements

The authors gratefully acknowledge the financial support from the Department of Science and Technology (DST), South Africa under Biocomposite Centre of Competence (BCoC) programme. Swedish Research Council, (VR) under SIDA project 348-2008-6009 and the National Research Foundation (NRF) under SIDA project UID: 68745 are acknowledged for collaboration funds.

References

Brent, A. C., Rohwer, M. B., Friedrich, E., & Von Blottnitz, H. (2002). Status of life cycle assessment and engineering research in South Africa. *International Journal of Life Cycle Assessment*, *7*(3), 167–172.

Cao, X., Dong, H., & Li, C. M. (2007). New nanocomposite materials reinforced with flax cellulose nanocrystals in waterborne polyurethane. *Biomacromolecules*, *8*, 899–904.

Chen, Y., Liu, C., Chang, P. R., Cao, X., & Anderson, D. P. (2009). Bionanocomposites based on pea starch and cellulose nanowhiskers hydrolyzed from pea hull fibre: Effect of hydrolysis time. *Carbohydrate Polymers*, *76*(4), 607–615.

Du Plessiss, J. (2003). *Maize production*. ⟨http://www.cd3wd.com/CD3WD_40/LSTOCK/001/SA_InfoPaks/docs/maizeproduction.pdf⟩

Dufresne, A. (2012). *Nanocellulose: From nature to high performance tailored materials*. Berlin/Boston: Walter de Gruyter GmbH.

Fahma, F., Iwamoto, S., Hori, N., Iwata, T., & Takemura, A. (2011). Effect of pre-acid-hydrolysis treatment on morphology and properties of cellulose nanowhiskers from coconut husk. *Cellulose*, *18*, 443–450.

Fukuzumi, H., Saito, T., & Isogai, A. (2013). Influence of TEMPO-oxidized cellulose nanofibril length on film properties. *Carbohydrate Polymers*, *93*, 172–177.

Haafiz, M. K. M., Eichhorn, S. J., Hassan, A., & Jawaid, M. (2013). Isolation and characterization of microcrystalline cellulose from oil palm biomass residue. *Carbohydrate Polymers*, *93*, 628–634.

Henriksson, M., Berglund, L. A., Isaksson, P., Lindström, T., & Nishino, T. (2008). Cellulose nanopaper structures of high toughness. *Biomacromolecules*, *9*, 1579–1585.

Henrique, M. A., Silvério, H. A., Neto, W. P. F., & Pasquini, D. (2013). Valorization of an agro-industrial waste, mango seed, by the extraction and characterization of its cellulose nanocrystals. *Journal of Environmental Management*, *121*, 202–209.

Huang, X., & Netravali, A. (2009). Biodegradable green composites made using bamboo micro/nano-fibrils and chemically modified soy protein resin. *Composites Science and Technology*, *69*, 1009–1015.

Iwatake, A., Nogi, M., & Yano, H. (2008). Cellulose nanofiber-reinforced polylactic acid. *Composites Science and Technology*, *68*, 2103–2106.

Kargarzadeh, H., Ahmad, I., Abdullah, I., Dufresne, A., Zainudin, S. Y., & Sheltami, R. M. (2012). Effects of hydrolysis conditions on the morphology, crystallinity, and thermal stability of cellulose nanocrystals extracted from kenaf bast fibers. *Cellulose*, *19*, 855–866.

Li, R., Fei, J., Cai, Y., Li, Y., Feng, J., & Yao, J. (2009). Cellulose whiskers extracted from mulberry: A novel biomass production. *Carbohydrate Polymers*, *76*, 94–99.

Miao, Q., Chen, L., Huang, L., Tian, C., Zheng, L., & Ni, Y. (2014). A process for enhancing the accessibility and reactivity of hardwood kraft-based dissolving pulp for viscose rayon production by cellulose treatment. *Bioresource Technology*, *154*, 109–113.

Missoum, K., Martoïa, F., Belgacem, M. N., & Bras, J. (2013). Effect of chemically modified nanofibrillated cellulose addition on the properties of fiber-based materials. *Industrial Crops and Products*, *48*, 98–105.

Neto, W. P. F., Silvério, H. A., Oliveira, N., & Pasquini, D. (2013). Extraction and characterization of cellulose nanocrystals from agro-industrial residue—Soy hulls. *Industrial Crops and Products*, *42*, 480–488.

Oksman, K., Etang, J. A., Mathew, A. P., & Jonoobi, M. (2011). Cellulose nanowhiskers separated from a bio-residue from wood bioethanol production. *Biomass and Bioenergy*, *35*, 146–152.

Qing, Y., Sabo, R., Zhu, J. Y., Agarwal, U., Cai, Z., & Wu, Y. (2013). A comparative study of cellulose nanofibrils disintegrated via multiple processing approaches. *Carbohydrate Polymers*, *97*, 226–234.

Rosa, M. F., Medeiros, E. S., Malmonge, J. A., Gregorski, K. S., Wood, D. F., Mattoso, L. H. C., et al. (2010). Cellulose nanowhiskers from coconut husk fibers: Effect of preparation conditions on their thermal and morphological behavior. *Carbohydrate Polymers*, *81*(1), 83–92.

Rosli, N. A., Ahmad, I., & Abdullah, I. (2013). Isolation and characterization of cellulose nanocrystals from agave angustifolia fibre. *Bioresource*, *8*, 1893–1908.

Satyamurthy, P., & Vigneshwaran, N. (2013). A novel process for synthesis of spherical nanocellulose by controlled hydrolysis of microcrystalline cellulose using anaerobic microbial consortium. *Enzyme and Microbial Technology*, *52*, 20–25.

Segal, L., Greely, J. J., Martin, A. E., & Conrad, C. M. (1959). An empirical method for estimating the degree of crystallinity of native cellulose using X-ray diffractometer. *Textile Research Journal*, *29*, 786–794.

Sehaqui, H., Liu, A., Zhou, Q., & Berglund, L. A. (2010). Fast preparation procedure for large, flat cellulose and cellulose/inorganic nanopaper structures. *Biomacromolecules*, *11*, 2195–2198.

Sheltami, R. M., Abdullah, I., Ahmad, I., Dufresne, A., & Kargarzadeh, H. (2012). Extraction of cellulose nanocrystals from mengkuang leaves (*Pandanus tectorius*). *Carbohydrate Polymers*, *88*, 772–779.

Siqueira, G., Tapin-Lingua, S., Bras, J., Perez, D. S., & Dufresne, A. (2010). Morphological investigation of nanoparticles obtained from combined mechanical shearing, and enzymatic and acid hydrolysis of sisal fibers. *Cellulose*, *17*, 1147–1158.

Silvério, H. A., Neto, W. P. F., Dantas, N. O., & Pasquini, D. (2013). Extraction and characterization of cellulose nanocrystals from corncob for application as reinforcing agent in nanocomposites. *Industrial Crops and Products*, *44*, 427–436.

Wang, H., Li, D., & Zhang, R. (2013). Preparation of ultralong cellulose nanofibres and optically transparent nanopapers derived from waste corrugated paper pulp. *Bioresources*, *8*(1), 1374–1384.

Wu, Q., Meng, Y., Concha, K. E., Wang, S., Li, Y., Ma, L., et al. (2013). Influence of temperature and humidity on nano-mechanical properties of cellulose nanocrystal films made from switchgrass and cotton. *Industrial Crops and Products*, *48*, 28–35.

Yousefi, H., Faezipour, M., Hedjazi, S., Mousavi, M. M., Azusa, Y., & Heidari, A. H. (2013). Comparative study of paper and nanopaper properties prepared from bacterial cellulose nanofibers and fibers/ground cellulose nanofibers of canola straw. *Industrial Crops and Products*, *43*, 732–737.

Zhao, J., Zhang, W., Zhang, X., Zhang, X., Lu, C., & Deng, Y. (2013). Extraction of cellulose nanofibrils from dry softwood pulp using high shear homogenization. *Carbohydrate Polymers*, *97*(2), 695–702.